American Journal of Chemistry 2025, 15(1): 1-9
DOI: 10.5923/j.chemistry.20251501.01

Reactivity Analyzing of Some Benzimidazole Derivatives in Inhibiting Aluminum Corrosion in Nitric Acid Solution

Toure Hadja Rokia[1], Mougo Andre Tigori[2,*], Aphouet Aurelie Koffi[1], Paulin Marius Niamien[1]

[1]Matter Constitution and Reaction Laboratory, Training and Research Unit for the Sciences of Matter Structures and Technology, University of Felix Houphouet Boigny, Abidjan, Côte d'Ivoire
[2]Environmental Sciences and Technologies Laboratory, Environmental Training and Research Unit, University of Jean Lorougnon Guede, Daloa, Côte d'Ivoire

Abstract Gravimetric tests, density functional theory (DFT) and quantitative structure-property relationship (QSPR) calculations were employed to study three benzimidazole derivatives reactivity in inhibiting aluminum corrosion in nitric acid media. These compounds are: 2-(((4-chlorobenzyl) thiol) methyl) -1H-benzo[d]imidazole (2-4-CBTM1HBI), 2-(((4-chlorobenzyl) thio) methyl) 1-H benzo[d] imidazole(M-4 1HBI-2MTMB) and 2-((benzylthio) methyl) 1-H benzo[d] imidazole (2-BTM1HBI). Experimental data at 298K and Cinh= 5. 10^{-3}M indicate that the inhibitory efficiencies of 2-4-CBTM1HBI, M-4 1HBI-2MTMB and 2-BTM1HBI are 97.74%, 98.51% and 96.09% respectively. These values show that the compound M-4 1HBI-2MTMB has the best inhibition performance. DFT calculations of quantum chemical descriptors in 6-311++G (d, p) basis with B3LYP functional clearly explained how each molecule inhibits aluminum corrosion in the solution studied. Which theoretical parameters support the good inhibition efficiency of M-4 1HBI-2MTMB. The statistical results of the QSPR (Quantitative Structure-Activity Relationship) model indicate that the set of parameters (ΔN, ω, χ) provides a robust relationship between theoretical and experimental data. Thus, the theoretical approach used in this study is in line with the available experimental results.

Keywords Gravimetric tests, Density functional theory, Quantitative Structure-Activity Relationship, Benzimidazole derivatives, Inhibiting aluminum corrosion

1. Introduction

Corrosion is a natural phenomenon which strongly affects metals, leading to frequent repair and maintenance requirements in various industrial sectors. Maintenance operations are often aimed at extending the life of metal equipment, although their effectiveness is limited over time [1]. As a result, the protection of metals and alloys against corrosion becomes essential to reduce the need for frequent repairs. This protection requires the adoption of techniques adapted to each type of metal or alloy and to specific environmental conditions. Aluminum, widely used because of its excellent properties, is particularly prone to the formation of scale on its surface. Tartar, a product of corrosion, adversely affects the performance of metal equipment, making regular descaling and cleaning with acid solutions necessary. To guarantee the durability of such equipment and minimize metal dissolution in acid solutions, the use of corrosion inhibitors is increasingly recommended [2-4]. These inhibitors, often organic compounds, act by slowing down corrosion by forming a protective layer on metals, or by modifying the environment to make it less favorable to corrosion [6]. They can be added directly to corrosive media or incorporated into surface treatment products such as paints. Current research is focusing on the discovery of environmentally-friendly and effective inhibitors, combining experimental and theoretical approaches [7-9]. Among these approaches, density functional theory (DFT) has shown itself to be a promising method for better understanding the reactivity of organic molecules [10]. Indeed, DFT offers detailed information on the interactions between an inhibitor and the metal surface, while explaining the actual behavior of the inhibitor in contact with the metal [11,12]. Studies have shown that various organic compounds can inhibit metal corrosion using this theoretical approach, which is based on quantum chemistry [13,14]. DFT provides data on the electronic properties of inhibitors and their ability to adsorb to metal surfaces [15]. The computational descriptors obtained by this method can be used to characterize the reactivity of inhibitors and provide an in-depth explanation of their inhibition mechanism. This characterization, based on the quantitative structure-property relationship (QSPR), enables experimental research to be directed and new, more effective molecules

* Corresponding author:
tigori20@yahoo.fr (Mougo Andre Tigori)
Received: Dec. 13, 2024; Accepted: Jan. 10, 2025; Published: Jan. 21, 2025
Published online at http://journal.sapub.org/chemistry

to be synthesized. The aim of this study is to investigate the reactive properties of three benzimidazole derivatives in the inhibition of aluminum corrosion, in 1M nitric acid medium, using gravimetric, DFT and QSPR methods. The specific aim is to compare experimental data with theoretical results and to determine the quantum chemical parameters capable of linking these different data.

2. Experimental Part

2.1. Gravimetric Experiments

The aluminum samples, cylindrical in shape (1 cm in height and 0.25 cm in diameter), were carefully polished with abrasive paper of decreasing grit size, ranging from 40 to 600. After sanding, they were rinsed with distilled water, then cleaned in an acetone solution before being rinsed again with distilled water. The samples were then dried in an oven at 80°C. Once dried, each sample was weighed. Each pretreated sample was then immersed in 50 mL of 1M nitric acid solution, with or without inhibitor, for one hour. After this period, the samples were removed from the solution, dried again, then weighed. Experiments were carried out at a temperature of 298 K and an inhibitor concentration of 5 × 10-3 M. These conditions were chosen as they enabled optimum inhibition efficiency values to be obtained in the gravimetric tests.

Three molecules used in this work were synthesized and characterized by a team at Organic Chemistry and Natural Synthesis Laboratory, Felix Houphouët Boigny University. The characteristics of these compounds are listed in table 1.

The corrosion rate (W), aluminum recovery rate (θ) and inhibition efficiency of each inhibitor (IE(%)) are expressed from the following expressions [16]:

$$W = \frac{\Delta m}{S_e.t} = \frac{m_1 - m_2}{S_e.t} \quad (1)$$

$$\theta = \frac{W_0 - W}{W_0} \quad (2)$$

Where:

W_0: corrosion rate in the absence of inhibitor;

W: corrosion rate in the presence of inhibitor.

$$IE(\%) = \frac{W_0 - W}{W_0} \times 100 \quad (3)$$

2.2. DFT Calculations

DFT calculations were performed using Gaussian 03 [17] with the B3LYP (Becke, three parameter, Lee-Yang-Parr exchange correlation function) [18,19]. The molecular structures of the inhibitors were geometrically optimized using DFT.

These calculations were performed in the bases 6-31G (d), 6-31+G (d,p) and 6-311++G (d,p). Global reactivity quantum chemical parameters such as highest occupied orbital energy (EHOMO), lowest vacant orbital energy (ELUMO), energy gap (ΔE), dipole moment(μ), electronegativity (χ), hardness (η), softness (S), electrophilicity index (ω), electroaccepting power (ω^+) (omega at power plus close parenthesis and electrodonating power (ω^-) were calculated. The expressions used to access these quantities are given as follows [20-24]:

$$\Delta E = E_{\mathrm{LUMO}} - E_{HO\mathrm{MO}} \quad (4)$$

$$I = -E_{HOMO} \quad (5)$$

$$A = -E_{\mathrm{LUMO}} \quad (6)$$

Table 1. Molecular structure and gross formula of inhibitors

Names	Gross Formula	Molecular structure
2-((benzylthio) methyl) 1-H benzo[d] imidazole (2-BTM1HBI)	$C_{15}H_{14}N_2S$	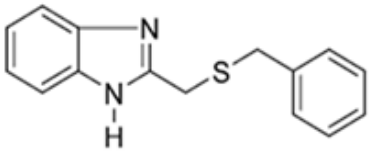
2-(((4-chlorobenzyl) thio) methyl) 1-H benzo[d] imidazole (M-4 1HBI-2MTMB)	$C_{17}H_{16}N_2O_2S$	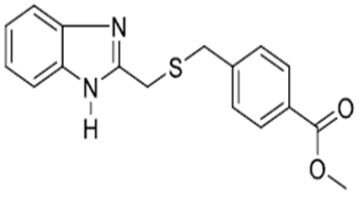
2-((((4-chlorobenzyl)thiol)methyl)-1H-benzo[d]imidazole (2-4-CBTM1HBI)	$C_{15}H_{23}N_2SCl$	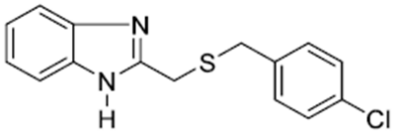

$$\chi = \frac{I+A}{2} = -\frac{E_{LUMO}+E_{HOMO}}{2} \quad (7)$$

$$\eta = \frac{I-A}{2} = \frac{E_{LUMO}-E_{HOMO}}{2} \quad (8)$$

$$\sigma = \frac{1}{\eta} = \frac{2}{I-A} \quad (9)$$

$$\Delta N = \frac{\chi_{Al}-\chi_{inh}}{2(\eta_{Al}+\eta_{inh})} \quad (10)$$

In this case χ_{Al} and χ_{inh} denote the absolute electronegativity of copper and inhibitor molecule respectively. The calculations were performed using the following theoretical values: $\chi_{Al} = 4.28\ eV$ [25] and $\eta_{Al} = 0$ [25]

$$\omega = \frac{\mu_P^2}{2\eta} = \frac{(\mathrm{I+A})^2}{4(\mathrm{I-A})} \quad (11)$$

$$\omega^+ = \frac{(I+3A)^2}{16(I-A)} \quad (12)$$

$$\omega^- = \frac{(3I+A)^2}{16(I-A)} \quad (13)$$

2.3. Quantitative Structure-Property Relationship (QSPR) Simulation

Studying the inhibitory reactivity of a molecule also involves predicting the activity of analogous molecules in this domain. In this work, a quantitative structure-property relationship approach was applied to correlate the experimental inhibitory efficiencies of each molecule with the quantum chemical parameters obtained by DFT calculations [26,27]. This process is based on the model of Lukovits et al [28], which aims to identify a set of quantum chemical parameters capable of predicting theoretical inhibitory efficacy values from experimental data. The linear model used is based on the following relationship:

$$\mathrm{IE}_{calc}(\%) = \frac{[Ax_1+Bx_2+Dx_3+E]C_i}{1+[Ax_1+Bx_2+Dx_3+E]C_i} * 100 \quad (14)$$

Four inhibitor concentrations were used in the study: 100 µM, 500 µM, 1000 µM and 5000 µM. Sets of three parameters (x_1, x_2, x_3) were tested to analyze the data obtained. This approach results in a system of four equations with four unknowns: A, B, D and E. The aim is to determine the values of the coefficients A, B, D and E for each molecule, so that the theoretical inhibition efficiency corresponds as closely as possible to that measured experimentally. The calculations required to solve this system were carried out using EXCEL software.

3. Results and Discussion

3.1. Gravimetric Data Analysis

The evolution of inhibition efficiency (IE) as a function of each inhibitor is shown in Figure 1.

Figure 1 examination shows that compound M-4 1HBI-2MTMB has the highest inhibition efficiency value at 298K and concentration C_{inh} = 5.10^{-3}M. This high performance reveals that M-4 1HBI-2MTMB absorbs strongly on aluminum surface at low temperatures.

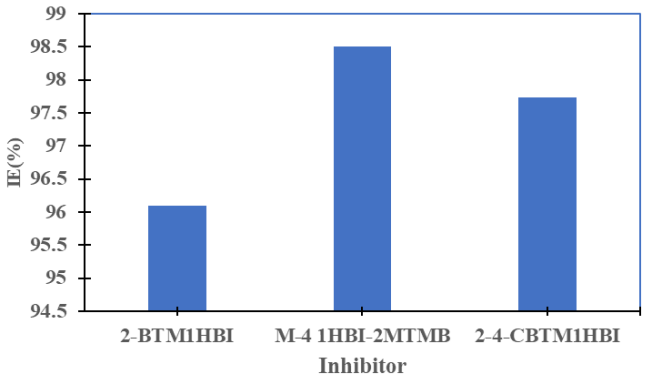

Figure 1. IE versus inhibitor at 298K and 5. 10^{-3}M

3.2. Theoretical Data Analysis

3.2.1. Choosing the Right Calculation Basis

Appropriate base choice base was made on basis calculation time and energy gap value. Calculations were performed in three different bases: 6-31G (d, p), 6-31+ G (d, p) and 6-311++G (d, p). The evolution of calculation time and energy gap (ΔE) are shown in Figures 2 and 3 respectively.

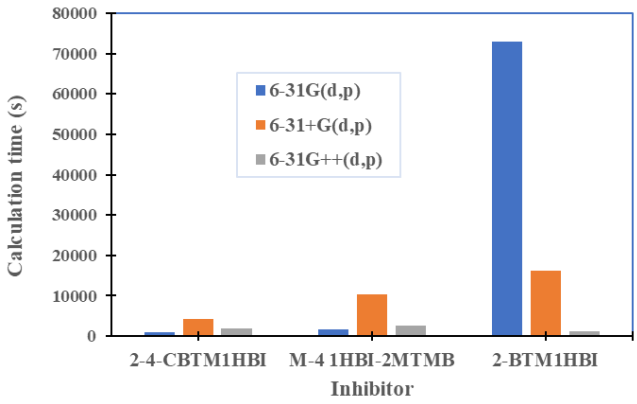

Figure 2. Theoretical computations time versus basis set for each inhibitor

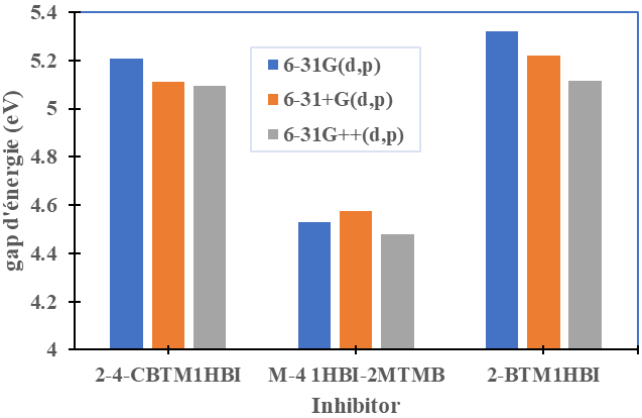

Figure 3. Energie gap (ΔE) versus basis set for each inhibitor

Analysis of Figures 2 and 3 shows that, for all molecules, the computation time and energy gap are relatively lower for the basis set 6-311++G (d, p) than for 6-31G and (d, p), 6-31+ G (d,p). The 6-311++G (d, p) basis will therefore be

used to calculate the other quantum chemical parameters. In fact, this triple Zeta basis with diffuse functions enables us to better describe the anisotropic distribution of electrons in space, and to obtain reliable results.

3.2.2. Global Reactivity of Inhibitors

Quantum chemical parameters calculations of each inhibitor were based on structures optimized in 6-311++G (d, p) basis with B3LYP functional. These optimized structures are shown in Figure 4. Table 2 shows the global reactivity parameter values obtained in the 6-311++G (d, p) basis with the B3LYP functional.

The ability of an organic compound to readily donate its electrons to a suitable acceptor depends on its highest occupied molecular orbital energy value (E_{HOMO}). Indeed, a high E_{HOMO} value reveals the compound's good ability to supply electrons to any suitable acceptor [29]. The E_{HOMO} values obtained for the compounds studied are in the order:

E_{HMO}(2-BTM1HBI)>E_{HOMO}(2-4-CBTM1HBI)>E_{HOMO}(M-41HBI-2MTMB). This order suggests that the 2-BTM1HBI compound is more inclined to donate electrons to aluminum, so it would imbibe more than the other two compounds. These theoretical data do not agree with the experimental results. Furthermore, the lowest vacant molecular orbital energy values of the compounds are in the order:

E_{LUMO}(2-BTM1HBI)> E_{LUMO}(2-4-CBTM1HBI) > E_{LUMO} (M-41HBI-2MTMB). According to the literature, any compound with a low E_{LUMO} value is more likely to receive electrons [29,30]. These results confirm that the good inhibition performance of M-41HBI-2MTMB obtained experimentally stems from its ability to receive electrons from aluminum.

2-4-CBTM1HBI

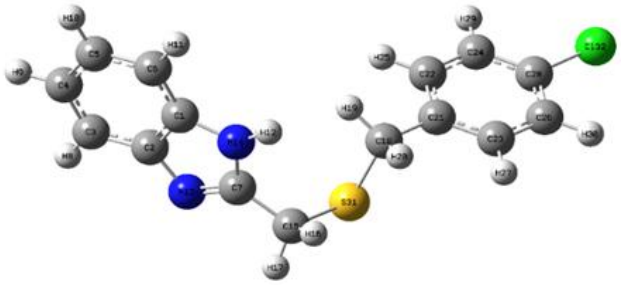

M-41HBI-2MTMB

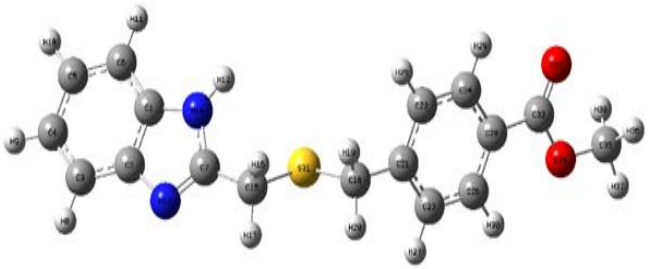

2-BTM1HBI

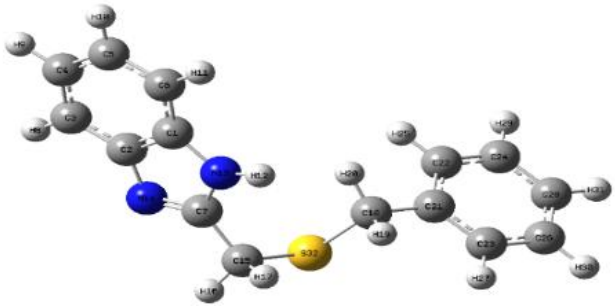

Figure 4. Optimized structures for different inhibitors

Table 2. Global reactivity parameter values for the inhibitors studied

Quantum chemical parameters	2-4-CBTM1HBI	M-41HBI-2MTMB	2-BTM1HBI
E_{HOMO} (eV)	-6.338	-6.368	-6.302
E_{LUMO} (eV)	-1.242	-1.890	-1.080
Energy gap ΔE (eV)	5.096	4.478	5.222
Dipole moment μ (D)	4.304	1.997	3.580
Ionization energy *I* (eV)	6.338	6.368	6.302
Electron affinity *A* (eV)	1.242	1.890	1.080
Electronegativity χ (eV)	3.790	4.129	3.691
Hardness η (eV)	2.548	2.239	2.611
Softness (σ) $(eV)^{-1}$	0.392	0.447	0.383
Fraction of electron transferred ΔN	0.096	0.247	0.226
Electrophylicity index ω	2.819	3.807	2.609
Electroaccepting power ω^+	1.242	2.022	1.089
Electrodonating power ω^-	5.032	6.152	4.781
Total energy E_T (Ha)	-1547.562	-1315.889	-1087.942

This exchange of electrons between each inhibitor and the metal indicates the formation of covalent bonds. The electron distribution at each molecular orbital is illustrated in Figure 5.

The ionization energy (I) and electron affinity (A) values show that there is a strong interaction between each inhibitor and the metal [30].

As for the energy gap (ΔE) values, they are in the following order: ΔE(M-41HBI-2MTMB) < ΔE(2-4-CBTM1HBI) < ΔE(2-BTM1HBI). The lower ΔE is, the more exchanges between molecule and metal are favored for each inhibitor [31,32].

The values obtained indicate that the various molecules are reactive, as the energy required to remove an electron from the last occupied orbital will be low. The compound M-41HBI-2MTMB, which has the lowest value, has excellent inhibition activity compared with the other two. This excellent reactivity is due to the presence of several heteroatoms (N, O, S).

These heteroatoms are the basis for electronic exchanges between the metal and the inhibitor. This result is in line with the experimental data obtained.

According to some authors, low values of dipole moment (μ) favor the accumulation of inhibitor molecules on the metal surface, thus increasing inhibition efficiency [33,34] This suggests that the high inhibition efficiencies obtained can be justified by these low values of the molecule's dipole moment. Compound M-41HBI-2MTMB has the highest value for softness (σ) and the lowest value for hardness (η). These values indicate that this molecule is soft and reacts readily with aluminum to form a complex capable of reducing the dissolution of the metal in the solution studied [35]. These theoretical data are in line with experimental tests.

The positive values for the fraction of electrons transferred and electronegativity describe the electron transfer between each inhibitor and the metal. The order N(M-41HBI-2MTMB)>ΔN(2-BTM1HBI) >ΔE(2-4-CBTM1HBI) obtained from the theoretical values justifies the good inhibition action of the molecules studied. Consequently, M-41HBI-2MTMB is the best inhibitor [36].

The high values of the electrophilicity index (ω) obtained relate to the electrophilic character of each inhibitor [29]. In this case, the compounds studied are more likely to readily accept electrons from the metal or would readily undergo nucleophilic attack. In addition, the electron acceptor value of electroaccepting power ω+ of each inhibitor is closer to electron affinity values (A). This proximity confirms the electrophilic nature of the inhibitors studied [37].

The negative total energy (E_T) values indicate a strong interaction between each inhibitor and aluminum, highlighting the ease of electronic transactions between the two species [38].

Inhibitors	Orbital HOMO	Orbital LUMO
2-4-CBTM1HBI	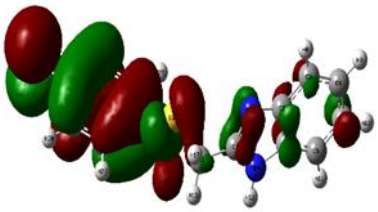	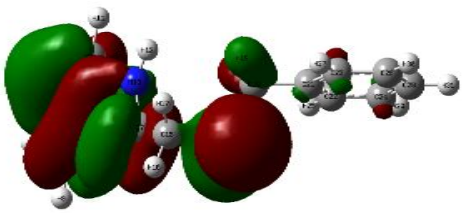
M-41HBI-2MTMB	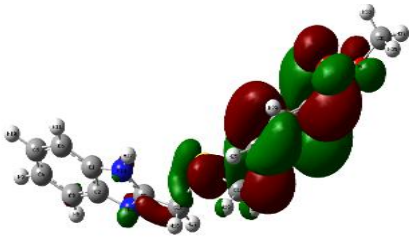	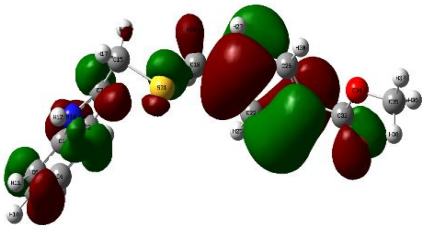
2-BTM1HBI	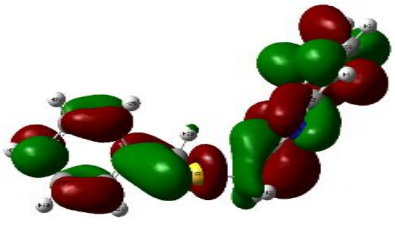	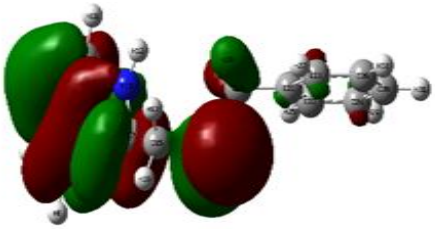

Figure 5. Electron distribution density of HOMO and LUMO orbitals by B3LYP/6-311++G (d)

3.2.3. Quantitative Structure-Property Relationship Calculation Analyzing

The correlation between experimental and theoretical values was carried out using quantitative structure-property relationship (QSPR) method [39]. For this approach, experimental values measured at 298 K were used. Several sets of parameters were tested for each inhibitor. We selected the sets for which the inhibition efficiency values obtained were closest to the experimental values. The calculated coefficient values A, B, C and D are listed in Table 3. Figures 6, 7, 8 show the different correlations between experimental and theoretical data for each inhibitor.

Table 3. Values of coefficients A, B, C and D

Inhibitor	Set of parameters	A	B	D	E
2-4-CBTM1HBI	(E_{HOMO},ΔE,E_{LUMO})	-1456.851	-1.8389X10^{13}	-6.2207 X10^{13}	1.645 X10^{13}
	(ΔN, ω, χ)	9439.87016	-648.750078	1.1627 X10^{14}	-4.5577X10^{13}
M-41HBI-2MTMB	(E_{HOMO}, ΔE, E_{LUMO})	1262.61476	5272.56772	2173.11234	-11463.0319
	(ΔN, ω, χ)	2.0669X10^{13}	1784.96747	-145.420485	-5.1052X10^{12}
2-BTM1HBI	(E_{HOMO}, ΔE, E_{LUMO})	-4.8009 X10^{11}	-5.2809 X10^{12}	-2.1597 X10^{13}	1.2263 X10^{12}
	(ΔN, ω, χ)	-267.335176	1042.44818	8.5466 X10^{12}	-3.1546X10^{13}

Table 4. R^2 values and statistical parameters

Inhibitor	Set of parameters	R^2	SSE	RMSE
2-4-CBTM1HBI	(E_{HOMO}, ΔE, E_{LUMO})	0.9301	519.94	11.3995
	(ΔN, ω, χ)	**0.9247**	**479.6077**	**10.9499**
M-41HBI-2MTMB	(E_{HOMO}, ΔE, E_{LUMO})	0.9564	1127.1361	16,7863
	(ΔN, ω, χ)	**0.9438**	**560.1205**	**11.8334**
2-BTM1HBI	(E_{HOMO}, ΔE, E_{LUMO})	0.9058	2678.24	25.8758
	(ΔN, ω, χ)	**0.9000**	**102.886**	**5.0716**

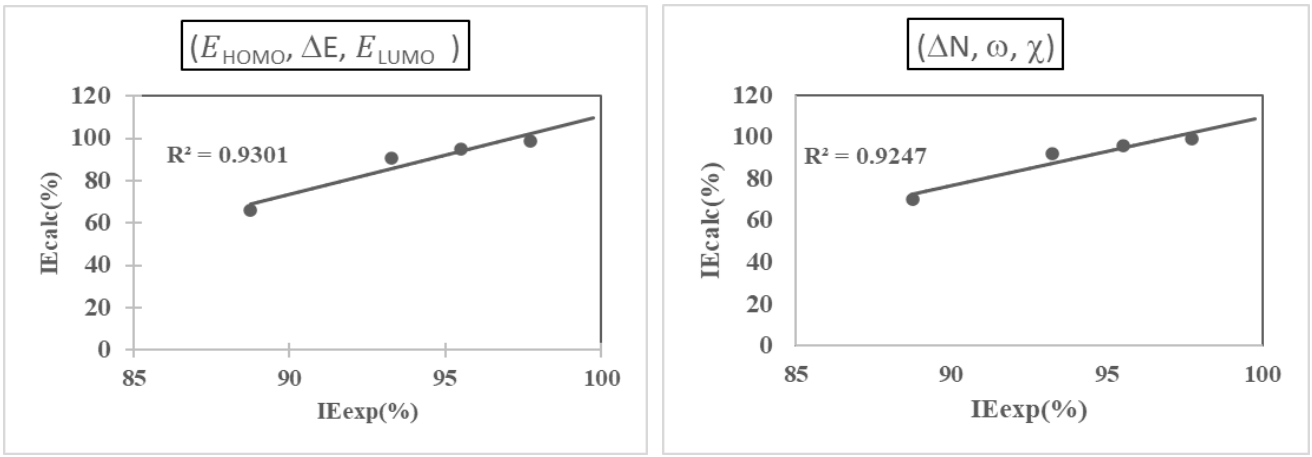

Figure 6. Experimental and theoretical inhibition efficiency correlation for 2-4-CBTM1HBI

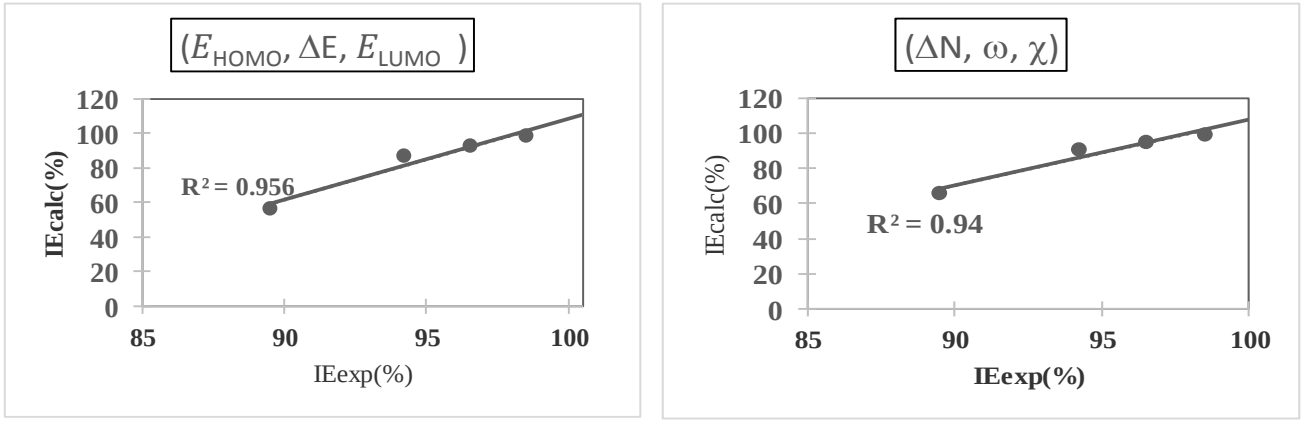

Figure 7. Experimental and theoretical inhibition efficiency correlation for M-41HBI-2MTMB

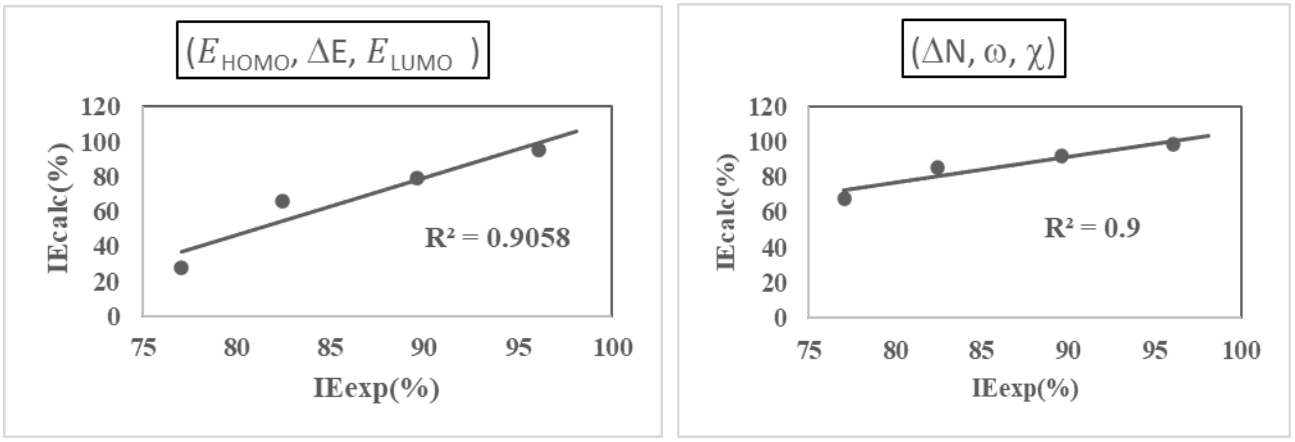

Figure 8. Experimental and theoretical inhibition efficiency correlation for 2-BTM1HBI

In order to validate this correlation from this model, statistical parameters are used to select the optimal set of descriptors, enabling a reliable relationship to be established from the available data. These parameters are determined from the following expressions [40]:

The sum of square errors (SSE):

$$SSE = \sum_{i=1}^{N} (IE_{exp} - IE_{calc})^2 \quad (15)$$

The root mean square error (RMSE):

$$RMSE = \sqrt{\frac{\sum_{i=1}^{N} (IE_{exp} - IE_{calc})^2}{N}} \quad (16)$$

The values of these parameters are listed in Table 4.

Analysis of Table 4 shows that the set of parameters (ΔN, ω, χ) has the lowest statistical parameter values. These data indicate that this parameter set can be used to correlate the experimental and theoretical inhibition efficiencies of 2-4-CBTM1HBI; M-41HBI-2MTMB; 2-BTM1HBI as well as analogous molecules.

4. Conclusions

In this work, the inhibition activities of three benzimidazole derivatives were evaluated using theoretical and experimental simulations. The key points summarizing this work are as follows:

- The three molecules studied display good reactivity in inhibiting aluminum corrosion in 1M nitric acid media, with the following order of inhibition performance: IE (%) (M-41HBI-2MTMB) >IE (%) (2-4-CBTM1HBI) > IE (%) (2-BTM1HBI).
- Theoretical data calculated in base 6-311++G (d, p) such that E_{HOMO} and ΔE follow the following order: E_{HMO}(2-BTM1HBI) > E_{HOMO}(2-4-CBTM1HBI) > E_{HOMO}(M-41HBI-2MTMB); ΔE(M-41HBI-2MTMB) < ΔE(2-4-CBTM1HBI) < ΔE(2-BTM1HBI) this confirms the compound M-41HBI-2MTMB has the better inhibition activity than the others.
- The set of parameters (ΔN, ω, χ) used to correlate the experimental and theoretical inhibition efficiencies of 2-4-CBTM1HBI; M-41HBI-2MTMB; 2-BTM1HBI as well as analogous molecules. This suggests that the model is capable of accurately reproducing or predicting behavior observed in the laboratory.
- The theoretical approach in agreement with the reported experimental data is a positive indicator of the validity and reliability of QSPR model in this specific context.

REFERENCES

[1] Arrousse, N., Fernine, Y., Haldhar, R., Berdimurodov, E., Hamza Ichou, Al-Zaqri, N., Mohammed, K., Seong-Cheol, K., Mustapha, T., 2023, Corrosion protection studies of different alloys in 1 M HCl by benzimidazole derivative: Combined molecular dynamic simulations/DFT, Journal of Environmental Chemical Engineering, 11(3), 109642.

[2] Caid, Z.A.E., Left, D.B., Thoume, A. *et al*., 2023, A Comprehensive Computational Study of N-Phenylacetamide Derivatives as Corrosion Inhibitors for Copper: Insights from DFT and Molecular Dynamics, Journal of Bio- and Tribo-Corrosion, 9, 83.

[3] Matine, A., Es-Sounni, B., Bakhouch, M. *et al.*, 2024, Design, synthesis, and evaluation of a pyrazole-based corrosion inhibitor: a computational and experimental study, Scientific Reports, 14, 25238.

[4] Da,Y., Liu, Y., Baimei, T., Tengda, M., Shihao, Z., Yazhen, W., Lei, G., Baohong, G., Yangang, H., 2021, Theoretical and electrochemical analysis on inhibition effects of benzotriazole derivatives (un- and methyl) on copper surface, Journal of Molecular Structure, 1243, 130871.

[5] Jinbo, J., Baimei, T., Shihao, Z., Tengda, M., Lei, G., Wei L., Mei, Y., Fangyuan, W., Haoyu, D., Xiaolong, W., 2022, Investigation on the control effect of benzotriazole and two derivatives on cobalt pitting corrosion in chemical mechanical polishing process: A combination of experiments and theoretical simulations, Journal of Molecular Liquids, 367, Part B, 120487.

[6] Abdelmalek, M., Mohamed, B., Haydar Mohammad-Salim, H., Abdallah, M. E., Ali H. *et al*., 2024, Exploring the synthesis and application of a pyrazole derivative in corrosion protection: Theoretical modeling and experimental investigations, Journal of Molecular Structure, 1312, Part 1, 138458.

[7] Madkour, L.H., Elshamy, I.H., 2016, Experimental and computational studies on the inhibition performances of benzimidazole and its derivatives for the corrosion of copper in nitric acid, International Journal of Industrial Chemistry 7, 195-221.

[8] Fouda, A.S., Ismail, M.A., Khaled, M.A. *et al.*, 2022, Experimental and computational chemical studies on the corrosion inhibition of new pyrimidinone derivatives for copper in nitric acid. Scientific Reports, 12, 16089.

[9] Deyab, M.A., AlGhamdi, J.M., Abdeen, M.M. *et al.* (2024), Chemical, electrochemical, and quantum investigation into the use of an organophosphorus derivative to inhibit copper corrosion in acidic environments. Scientific Reports, 14, 11395.

[10] Sourav, K. S., Abhiram, H., Naresh Chandra, M., Priyabrata, B., 2016, A comparative density functional theory and molecular dynamics simulation studies of the corrosion inhibitory action of two novel N-heterocyclic organic compounds along with a few others over steel surface, Journal of Molecular Liquids, 215, 486-495.

[11] Hsissou, R., About, S., Berisha A., Mohamed, B., Mohammed, A., Najat, H., Ahmed, E., 2019, Experimental, DFT and molecular dynamics simulation on the inhibition performance of the DGDCBA epoxy polymer against the corrosion of the E24 carbon steel in 1.0 M HCl solution, Journal of Molecular Structure, 1182, 340-351.

[12] Shahraki, M., Maryam, D., Shirin, E., 2016, Theoretical studies on the corrosion inhibition performance of three amine derivatives on carbon steel: Molecular dynamics simulation and density functional theory approaches, Journal of the Taiwan Institute of Chemical Engineers, 62, 313-321.

[13] Laihemdi, F., Barhoumi, A., Zarri, M. et al., 2024, Inhibition of corrosion of an aluminum alloy by rosemary and eucalyptus extracted oils in 1 M hydrochloric acid medium: an experimental and theoretical study, Environmental Science and Pollution Research, 31, 62147-62173.

[14] Anusuya, N., Saranya, J., Benhiba, F. *et al.*, 2022, Isoxazoline Derivatives as Inhibitors for Mild Steel Corrosion in 1M H_2SO_4: Computational and Experimental Investigations. Journal of Materials Engineering and Performance, 31, 7204–7219.

[15] Dahmani, K., Galai, M., Ouakki, M. *et al.* 2023, New Xanthene Diones Compounds as a Corrosion Inhibitor of Mild Steel in Acid Medium: Electrochemical, Surface Characterization and Theoretical Insights. Chemistry Africa, 6, 2049–2069.

[16] Sourav, K.S., Alokdut D., Pritam, G., Dipankar, S., Priyabrata, B., 2016, Novel Schiff-base molecules as efficient corrosion inhibitors for mild steel surface in 1 M HCl medium: experimental and theoretical approach; Physical Chemistry Chemical Physics, 18, 17898-17911.

[17] Frisch, M. J., Trucks, G. W., Schlegel, H. B. et al., 2003, Gaussian 03, Gaussian, Inc.: Pittsburgh P A.

[18] Becke, A.D. (1993) Density-Functional Thermochemistry. III. The Role of Exact Exchange. Journal of Chemical Physics, 98, 1372-1377.

[19] Lee, C., Yang, W. and Parr, R.G. (1988), Development of the Colle-Salvetti Correlation-Energy Formula into a Functional of the Electron Density, Physical Review B, 37, 785-789.

[20] Lei, G., Savaş Kaya, Ime Bassey, O., Xingwen, Z., Yujie, Q., 2017, Toward understanding the anticorrosive mechanism of some thiourea derivatives for carbon steel corrosion: A combined DFT and molecular dynamics investigation, Journal of Colloid and Interface Science, 506, 478-485.

[21] Shubhra, P., Deepti, J., Shamima, H., Amrita, B., Shrivastava, R., Saroj, K. P., Hemanta, K. K., Hassane L., Ill-Min C., Debasis B., 2019, A new insight into corrosion inhibition mechanism of copper in aerated 3.5 wt.% NaCl solution by eco-friendly Imidazopyridine Dye: experimental and theoretical approach, Chemical Engineering Journal, 358, 725-742.

[22] Beda, R. H. B., Niamien, P. M., Avo Bilé, E. B., Trokourey, A., 2017, Inhibition of Aluminum Corrosion in 1.0 M HCl by Caffeine: Experimental and DFT Studies, Hindawi Advances in Chemistry, 6975248.

[23] Tigori, M. A.; Kouyaté, A.; Kouakou, V.; Niamien, P. M.; Trokourey, A. 2020, Computational Approach for Predicting the Adsorption Properties and Inhibition of Some Antiretroviral Drugs on Copper Corrosion in HNO_3, European Journal of Chemistry., 11, 235-244.

[24] Garcia-Ochoa, E., Guzmán-Jiménez, S.J. Hernández, J.G., Pandiyan, T., Vásquez Pérez, J.M., Cruz-Borbolla, J., 2016, Journal of Molecular Structure, 1119, 314–324.

[25] Pearson RG., 1988, Absolute Electronegativity and Hardness: application to Inorganic Chemistry, Inorganic Chemistry, 27(4), 734-740.

[26] Tigori M.A, Koné A., Koua, N. R., Yeo M., Niamien, P.M., 2022, Copper corrosion inhibition in nitric acid solution by 2-(1,3-dihydrobenzimidazol-2-ylidene) -3-oxo-3-(pyridin-3-yl) propanenitrile: Gravimetric, Quantum chemical and QSPR studies. Mediterranean Journal of Chemistry, 12(2), 123-139.

[27] Quadri, T.W., Olasunkanmi, L. O., Fayemi, O. E., Lgaz, H., Dagdag, O., Sherif, E. M., Alrashdi, A. A., Akpan, E. D., Lee, H., Ebenso, E. E., 2022, Computational insights into quinoxaline -based corrosion inhibitors of steel in HCl: Quantum chemical analysis and QSPR-ANN studies, Arabian Journal of Chemistry, 15(7), 103870.

[28] Lukovits, I., Shaban, A., & Kalman, E. (2003). Corrosion inhibitors: Quantitative structure–activity relationships, Russian Journal of Electrochemistry, 39, 177-181.

[29] Khattabi, M., Benhiba, F., Tabti, S., Djedouani, A., El Assyry, A., Touzani, R., Warad, I., Oudda, H., Zarrouk, A., 2019, Performance and computational studies of two soluble pyran derivatives as corrosion inhibitors for mild steel in HCl, Journal of Molecular Structure, 1196, 231-244.

[30] Hsissou, R, About, S., Zaki, S., Fouad, B., Nuha Wazzan, N., Lei G., Nouneh, K., Samir, B., Hamid, E., Mohamed E.T., Mohammed, A., Ahmed, E., 2021, Synthesis and anticorrosive properties of epoxy polymer for CS in [1 M] HCl solution: Electrochemical, AFM, DFT and MD simulations, Construction and Building Materials, 270, 121454.

[31] Dagdag, O., El Harfi, A., Cherkaoui, O., Safi, Z., Wazzan, N., Guo, L., Akpan, E., Verma, C., Ebenso, E., Jalgham, R.T., 2019, Rheological, electrochemical, surface, DFT andmolecular dynamics simulation studies on the anticorrosive properties of newepoxy monomer compound for steel in 1 M HCl solution, RSC Advances, 9, 4454–4462.

[32] Dagdag, O., El Harfi, A., El Gouri, M., Safi, Z., Jalgham, R.T., Wazzan, N., Verma, C., Ebenso, E., Kumar, U.P., 2019, Anticorrosive properties of Hexa (3-methoxy propan-1, 2-diol)

cyclotri-phosphazene compound for carbon steel in 3% NaCl medium: gravimetric, electrochemical, DFT and Monte Carlo simulation studies, Heliyon, 5, e01340.

[33] Turuvekere, K. C., Kikkeri, N. M., Doddahosuru, M. G., Harmesh, C. T., 2016, Inhibition activity of new thiazole hydrazones towards mild steel corrosion in acid media by thermodynamic, electrochemical and quantum chemical methods, Journal of the Taiwan Institute of Chemical Engineers, 67, 521-531.

[34] Khattabi, F. Benhiba, S. Tabti, A. Djedouani, A. El Assyry, R. Touzani, I. Warad, H. Oudda, A. Zarrouk, 2019, Performance and computational studies of two soluble pyran derivatives as corrosion inhibitors for mild steel in HCl, Journal of Molecular Structure, 1196, 231-244.

[35] El Faydy, M., Benhiba, F., Lakhrissi, B., Ebn Touhami, M., Warad, I., Bentiss, F., Zarrouk, A., 2019, The inhibitive impact of both kinds of 5-isothiocyanatomethyl-8-hydroxyquinoline derivatives on the corrosion of carbon steel in acidic electrolyte, Journal of Molecular Liquids, 295, 111629.

[36] Lei, G., Savaş, K., Obot, I.B., Xingwen, Z., Yujie, Q., 2017, Toward understanding the anticorrosive mechanism of some thiourea derivatives for carbon steel corrosion: A combined DFT and molecular dynamics investigation, Journal of Colloid and Interface Science, 506, 478-485.

[37] Gazquez, J. L., Cedillo, A., Vela, A., 2007, Electrodonating and electroaccepting powers, The Journal of Physical Chemistry, 111, 1966-1970.

[38] Hegazy, M.A., Atlam, F.M., 2016, Three novel bolaamphiphiles as corrosion inhibitors for carbon steel in hydrochloric acid: Experimental and computational studies, Journal of Molecular Liquids, 218, 649-662.

[39] Mounir, G., Chtita S., Hmamouchi, R., Adad, A, Mohammed B., Lakhlifi T., 2016, The inhibitory activity of aldose reductase of flavonoid compounds: Combining DFT and QSAR calculations, Journal of Taibah University for Science, 10(4), 534-542.

[40] Masego, D., Lukman O. O., Omolola, E.F., Sasikumar, Y., Ramaganthan, B., Bahadur, I., Abolanle, S. A., Mwadham, M. K., Eno, E.E., 2015, Some Phthalocyanine and Naphthalocyanine Derivatives as Corrosion Inhibitors for Aluminium in Acidic Medium: Experimental, Quantum Chemical Calculations, QSAR Studies and Synergistic Effect of Iodide Ions, Molecules, 20, 15701-15734.